Biochemical Journal (2021) **478** 3741–3756
https://doi.org/10.1042/BCJ20210252

Research Article

BACH1, the master regulator of oxidative stress, has a dual effect on CFTR expression

Monali NandyMazumdar, Alekh Paranjapye, James Browne*, Shiyi Yin, Shih-Hsing Leir and Ann Harris

Department of Genetics and Genome Sciences, Case Western Reserve University, Cleveland, OH 44116, U.S.A

Correspondence: Ann Harris (ann.harris@case.edu)

The cystic fibrosis transmembrane conductance regulator (*CFTR*) gene lies within a topologically associated domain (TAD) in which multiple *cis*-regulatory elements (CREs) and transcription factors (TFs) regulate its cell-specific expression. The CREs are recruited to the gene promoter by a looping mechanism that depends upon both architectural proteins and specific TFs. An siRNA screen to identify TFs coordinating *CFTR* expression in airway epithelial cells suggested an activating role for BTB domain and CNC homolog 1 (BACH1). BACH1 is a ubiquitous master regulator of the cellular response to oxidative stress. Here, we show that BACH1 may have a dual effect on *CFTR* expression by direct occupancy of CREs at physiological oxygen (~8%), while indirectly modulating expression under conditions of oxidative stress. Hence BACH1, can activate or repress the same gene, to fine tune expression in response to environmental cues such as cell stress. Furthermore, our 4C-seq data suggest that BACH1 can also directly regulate *CFTR* gene expression by modulating locus architecture through occupancy at known enhancers and structural elements, and depletion of BACH1 alters the higher order chromatin structure.

Introduction

Misregulation of the mechanisms controlling gene expression may underlie many diseases. Accordingly, the identification of transcription factors (TFs) involved in key cellular processes may reveal therapeutic targets. Our focus is the transcriptional networks of human epithelial cells [1–3], which may be impaired in diseases of the lung and digestive system, among other tissues. One such disease is the life-limiting inherited disorder cystic fibrosis (CF), which is caused by mutations in the cystic fibrosis transmembrane conductance regulator (*CFTR*) gene. The *CFTR* locus is organized within a topologically associated domain (TAD) flanked by sites of CTCF and cohesin occupancy at −80.1 kb upstream and +48.9 kb downstream of the coding region of the gene [4–6]. Within this TAD, specific *cis*-regulatory elements (CREs) play critical roles by facilitating the recruitment of activating factors to the *CFTR* promoter, which in turn initiates cell-type-selective gene expression. In CFTR-expressing airway epithelial cell types, the intergenic CREs at −35 kb and −44 kb with respect to the transcription start site (TSS) are critical cell-type-selective enhancers [7] and their activity is likely dependent on a structural element at −20.9 kb [7,8]. The −35 kb CRE recruits key TFs [9] and also mediates looping between the *CFTR* promoter and the −80.1 TAD boundary [7]. In contrast, the −44 kb CRE may be stress responsive and harbors an antioxidant response element (ARE) at which the BTB and CNC homology 1, basic leucine zipper (BACH1) is bound along with v-Maf avian musculoaponeurotic fibrosarcoma oncogene homolog K (MafK), which together repress *CFTR*. Upon stimulation by sulforaphane, nuclear factor, erythroid 2-like 2 (NFE2L2 or NRF2) translocates into the nucleus, where it displaces BACH1 thus activating *CFTR* [10].

However, despite its repressive role at this site, in a replicated siRNA screen targeting ~1500 TFs in airway epithelial cells [2], BACH1 was identified as a *CFTR* activating factor, since its depletion

*Present address: Department of Pediatrics, Yale University School of Medicine, New Haven, CT, U.S.A.

Received: 7 April 2021
Revised: 30 September 2021
Accepted: 1 October 2021

Accepted Manuscript online: 4 October 2021
Version of Record published: 21 October 2021

© 2021 The Author(s). This is an open access article published by Portland Press Limited on behalf of the Biochemical Society and distributed under the Creative Commons Attribution License 4.0 (CC BY-NC-ND).

Biochemical Journal (2021) 478 3741–3756
https://doi.org/10.1042/BCJ20210252

caused a >1.6 fold reduction in CFTR mRNA levels. The observation that one TF may have opposite functions at different CREs is not unexpected and has been documented previously [11–13]. Moreover, a single TF can function both directly and indirectly at the same locus, by the recruitment of different cofactors. BACH1 is a ubiquitous master regulator of the oxidative stress response pathway [14]. Here, we determine how it impacts the *CFTR* locus and also controls the transcriptome of airway epithelial cells.

BACH1 belongs to the Cap'n'Collar type of basic region leucine zipper TF family (CNC-bZip) and also has BTB/POZ domains (broad complex, tram track, bric-a-brac/poxvirus and zinc finger) at the N-terminus. BACH factors bind to small Maf (sMaf) proteins and repress transcription by binding to the Maf recognition elements (MAREs) in genes [15]. BACH1 also provides a critical sensor of heme levels in the cell and combats oxidative stress, by repressing the heme oxygenase 1 (*HMOX1*) gene under physiological conditions. Upon exposure to oxidative stress, BACH1 translocates into the cytoplasm, while NRF2 dissociates from its cytoplasmic inhibitor, Kelch-like ECH-associated protein 1 (KEAP1), enters the nucleus and binds to MAREs along with small Maf proteins, thus activating its target stress response genes (reviewed in [14,16]). The NRF2/sMaf heterodimers bind at sites similar to the MAREs, which are both classified as types of ARE, (reviewed in [17]). BACH1 also directly regulates genes involved in the cell cycle, cell growth and proliferation, apoptosis and signal transduction [18,19], and may have roles in angiogenesis [20,21] and cancer [19,22–26].

Oxidative stress in the airway, generated by the release of excessive reactive oxygen species (ROS), causes lung damage in several diseases including asthma, chronic obstructive pulmonary disease (COPD) and lung cancer [27]. BACH1 represses the glutamate-cysteine ligase modifier (*GCLM*) subunit and glutamate-cysteine ligase catalytic (*GCLC*) subunit genes [18], which together encode the rate limiting glutathione (GSH) producing enzymes. GSH is the most abundant and important airway surface liquid antioxidant and is present at much higher concentrations than in other tissues [28]. Homeostasis of GSH in the airway surface liquid may alleviate the ROS induced damage evident in lung diseases including CF. Moreover, CFTR may function as one of the cellular efflux pumps for GSH [29]. In contrast, oxidative stress alone decreases CFTR mRNA and protein levels, apparently as an adaptive mechanism [30], while simultaneously up-regulating oxidative stress response genes such as *HMOX1* and *GCLC*. BACH1 may impact cellular responses to oxidative stress either by direct occupancy of gene promoters or CREs or through indirect mechanisms recruiting other proteins and TFs in its network. To determine the direct and indirect mechanisms of action of BACH1 genome wide in the airway epithelium we undertook RNA-sequencing upon siRNA-mediated depletion of BACH1 and chromatin immunoprecipitation with an antibody specific to BACH1 followed by deep sequencing (ChIP-seq), in two airway cell lines. The results identified redox regulation and the cell cycle as the major pathways directly regulated by BACH1. Furthermore, we identified the BACH1/NRF2 regulatory complex as pivotal in the protective role conferred by CFTR during oxidative stress. Our data also provide direct evidence of a key contribution of BACH1 and its interacting complex to higher order chromatin structure and looping, consistent with earlier work [31].

Results

An siRNA screen identifies BACH1 as a potential *CFTR* activator in airway epithelial cells

We previously described an siRNA screen for TFs that activate or repress *CFTR* expression in airway epithelial cells using the Dharmacon siGENOME siRNA library for human TFs [2]. Among potential CFTR activators, depletion of BACH1 was associated with a 2.12-fold reduction in normalized *CFTR* transcripts in Calu-3 cells. BACH1 is expressed in both Calu-3 [32] and primary human bronchial epithelial (HBE) [33] cells. We first validated the impact of BACH1 depletion on CFTR expression in Calu-3 cells using an siRNA from a different source (Ambion) than the siRNA library. The efficacy of the siRNA was demonstrated at the RNA level by RT-qPCR (Supplementary Figure S1A) and protein level by western blot with an antibody specific to BACH1 (Supplementary Figure S1B). CFTR expression in Calu-3 was reduced compared with negative control (NC) siRNA validating the results of the initial siRNA screen at the protein level (Figure 1A). The identification of BACH1 as an activator of *CFTR* in Calu-3 cells is in contrast with our earlier data in 16HBE14o$^-$ cells, where we showed repression of *CFTR* by BACH1 recruitment to an airway-selective enhancer at −44 kb upstream of the gene promoter. In 16HBE14o$^-$ cells, BACH1 normally occupies an ARE within this CRE, but is displaced by NRF2 under conditions of oxidative stress, to activate *CFTR* expression [10]. The observation that BACH1 has opposite effects in a lung adenocarcinoma cell line (Calu-3) and immortalized bronchial epithelial cells

© 2021 The Author(s). This is an open access article published by Portland Press Limited on behalf of the Biochemical Society and distributed under the Creative Commons Attribution License 4.0 (CC BY-NC-ND).

Biochemical Journal (2021) **478** 3741–3756
https://doi.org/10.1042/BCJ20210252

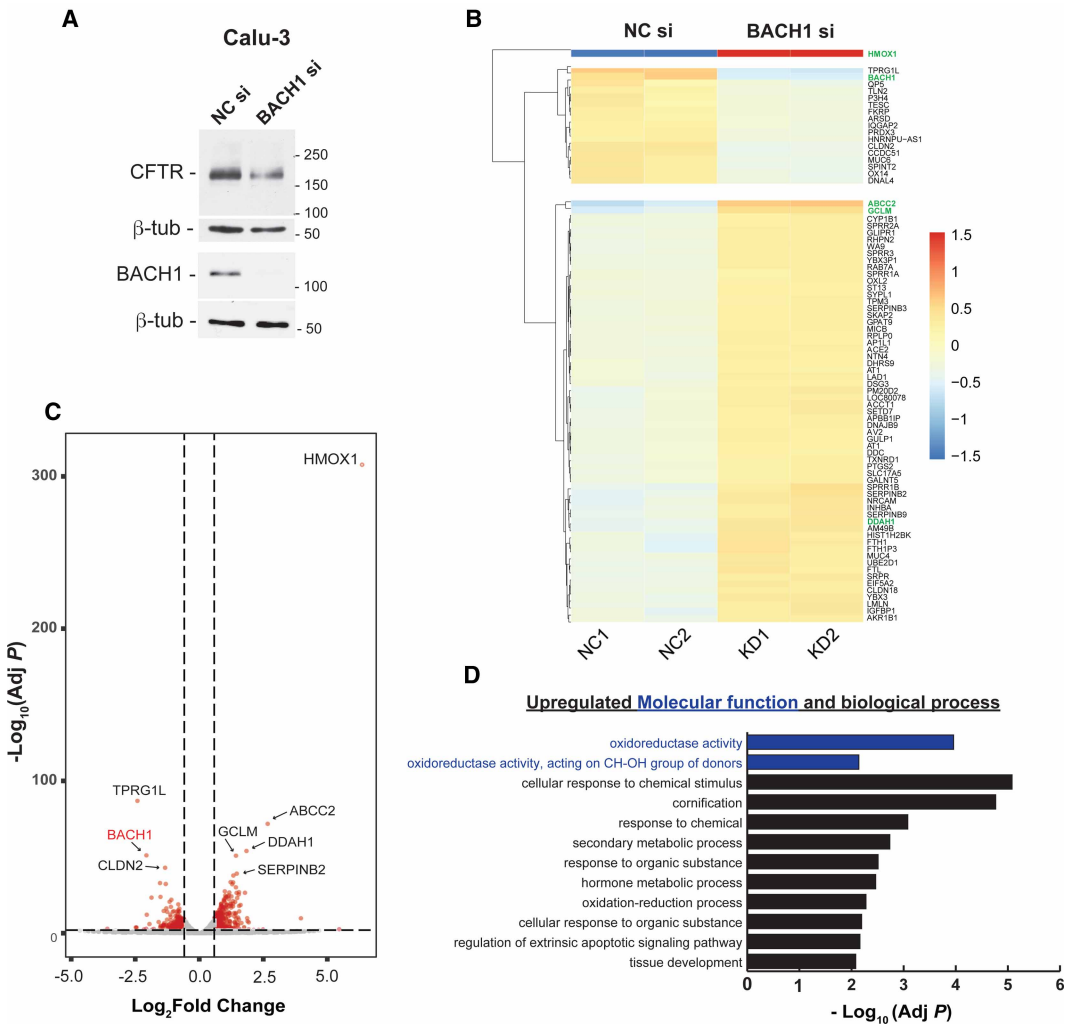

Figure 1. Depletion of BACH1 increases expression of oxidative response genes and decreases CFTR protein abundance.

(**A**) Western blot probed with antibodies specific to CFTR or BACH1 in Calu-3 cell lysates 72 h post-transfection with BACH1 or NC siRNAs. (**B**) Heat map of RNA-seq data showing the 80 most differentially expressed genes upon BACH1 depletion, (key genes are highlighted in green). (**C**) Volcano plot showing down (left) and up-regulated (right) genes with ≥1.5-fold change and an adjusted *P*-value of ≤0.01 after BACH1 depletion. (**D**) Gene ontology analysis denoting the most significant molecular functions (blue bars) and biological processes (black bars) by G:profiler [68] of the DEGs with a $\log_2$ fold change of >0.58 and <−0.58 with base mean above 30.

(16HBE14o$^-$) suggest a more complex role for this factor in regulating *CFTR* expression, possibly through both direct and indirect mechanisms.

BACH1 depletion in Calu-3 cells, up-regulates genes involved in oxidative stress response

Next, to determine the genome-wide functions of BACH1 in airway epithelial cells, we performed RNA-sequencing (RNA-seq) after siRNA-mediated depletion of BACH1 compared with a NC siRNA in Calu-3 cells. RNA-seq data were analyzed by DESeq2 to obtain estimates of transcript expression levels. A subset (80) of the most differentially expressed genes (DEGs), either up-regulated or down-regulated upon BACH1 depletion, are shown in a heatmap (Figure 1B). The DEGs were filtered to include only those with more than 1.5-fold change in expression and an adjusted *P*-value of 0.01 and used to generate a volcano plot (Figure 1C)

© 2021 The Author(s). This is an open access article published by Portland Press Limited on behalf of the Biochemical Society and distributed under the Creative Commons Attribution License 4.0 (CC BY-NC-ND).

Biochemical Journal (2021) 478 3741–3756
https://doi.org/10.1042/BCJ20210252

which validates BACH1 as one of the most down-regulated genes (also Supplementary Figure S1C). The volcano plot also shows that BACH1 is primarily a repressor of gene expression, since many more genes are up-regulated upon BACH1 depletion than are down-regulated (Supplementary Table S1). Furthermore, supporting the known role of BACH1 in regulating the oxidative stress response [18] *HMOX1* was the highest up-regulated DEG upon BACH1 depletion. A substantial increase in abundance of ATP-binding cassette subfamily C member 2 (*ABCC2*), *GCLM*, dimethylarginine dimethylaminohydrolase 1 (*DDAH1*) and serpin family B member 2 (*SERPINB2*) gene transcripts was also evident. Among down-regulated genes were tumor protein p63 regulated 1 like (*TPRG1L*) and Claudin 2 (*CLDN2*). A gene ontology process enrichment analysis was performed with g:Profiler [34] on the DEGs following BACH1 depletion (Figure 1D). The most enriched molecular function (MF) was oxidoreductase activity, while cellular response to chemical stimulus was the most enriched biological processes (BP) and includes among others the *ABCC2*, *DDAH1*, *HMOX1*, *GCLC*, *GLCM* genes, and those encoding several serpins and cytochrome p450. The *ABCC2* gene has an ARE, which is regulated by NRF2 in response to xenobiotic stress in the mouse liver [35]. DDAH1 enzyme controls oxidative stress and apoptosis via a miRNA pathway in mouse embryonic fibroblasts [36]. *HMOX1*, *GCLC*, *GCLM* are involved in the combat of oxidative stress and are directly targeted by BACH1 through binding to their MARE regions [18,37]. Serpins are protease inhibitors which play important roles in combating protease stress and modulate diseases of the lung [38,39] whilst most cytochrome p450 proteins are expressed in the lung and are involved in detoxification of carcinogens [40]. To confirm that our results were not limited to a single siRNA targeting BACH1 (Ambion, 4392420- S1860) we validated the effect of BACH1 depletion on 16HBE14o$^-$ cells with a pool of 3 siRNAs for BACH1 (Santa Cruz sc-37064). We chose 4 DEGs after BACH1 siRNA depletion from the RNA-seq data, and assayed their expression by RT-qPCR (Supplementary Figure S1D). *BACH1*, *HMOX1*, *DDAH1* and *GCLM* showed consistent changes with the RNA-seq and between siRNAs from the two sources; the expected elevation of ABCC2 was only observed with the Santa Cruz reagent; while *TPRG1L* was down-regulated by the Ambion siRNA as expected but slightly up-regulated by the Santa Cruz siRNA. These data validate the key observations of the RNA-seq experiment, but note minor variation in the response of individual genes. Overall, the results show that BACH1 controlled genes are involved in multiple oxidative stress response processes. We were unable to perform reliable rescue experiments, in which the effects of BACH1 depletion were reversed by overexpression of plasmid-derived BACH1, since the siRNAs used in the RNA-seq and validation experiments all target the coding region of BACH1.

The impact of BACH1 depletion is magnified by oxidative stress in airway epithelial cells

Since others reported previously that oxidative stress represses *CFTR* expression and function [30] and we show here that BACH1 depletion up-regulates oxidative stress response genes [18], we next asked if BACH1 inhibition in combination with H_2O_2-mediated oxidative stress would have competitive or additive effects on *CFTR* expression. The optimal concentration of H_2O_2 and exposure time required to induce oxidative stress in Calu-3 and 16HBE14o$^-$ cells, without inducing cell death, was determined [41,42]. Cell viability at different H_2O_2 concentrations and exposure times was measured by MTS assay (Supplementary Figure S2), and induction of oxidative stress was assayed by induction of *HMOX1* gene expression [43]. 16HBE14o$^-$ cells were more sensitive to H_2O_2 than Calu-3 cells, though assays were performed in both cell lines, using H_2O_2 concentrations of 800 μM for 15 h in Calu-3 cells and 600 μM for 8 h in 16HBE14o$^-$.

First, we focused on the expression of the *HMOX1* and *GCLM* genes, which were among the most up-regulated DEGs upon BACH1 depletion, evaluating after BACH1 knockdown or H_2O_2 stress alone or in combination. Calu-3 and 16HBE14o$^-$ cells were exposed to stress in serum-free media 48 h after siRNA-mediated depletion of BACH1, and gene expression measured by RT-qPCR (Figure 2). Effective depletion of BACH1 was evident in both cell lines. H_2O_2 stress alone significantly increased *BACH1* levels in Calu-3 but not 16HBE14o$^-$ cells (Figure 2A,B left panels). *HMOX1* transcript abundance increased upon H_2O_2 exposure in both cell lines, though to a lesser extent than upon BACH1 depletion. The greatest increase was seen when both treatments were combined (Figure 2A,B, middle panels). These results in airway epithelial cells are consistent with earlier observations in keratinocytes [44]. As expected, *GCLM* mRNA levels were significantly up-regulated by both BACH1 depletion and H_2O_2 stress alone in both cell lines, though the combined treatment was significantly different only in Calu-3 cells (Figure 2A,B, right panels). BACH1, HMOX1 and GCLM proteins were quantified by western blot of lysates from Calu-3 cells and these corresponded to transcript levels

© 2021 The Author(s). This is an open access article published by Portland Press Limited on behalf of the Biochemical Society and distributed under the Creative Commons Attribution License 4.0 (CC BY-NC-ND).

Biochemical Journal (2021) **478** 3741–3756
https://doi.org/10.1042/BCJ20210252

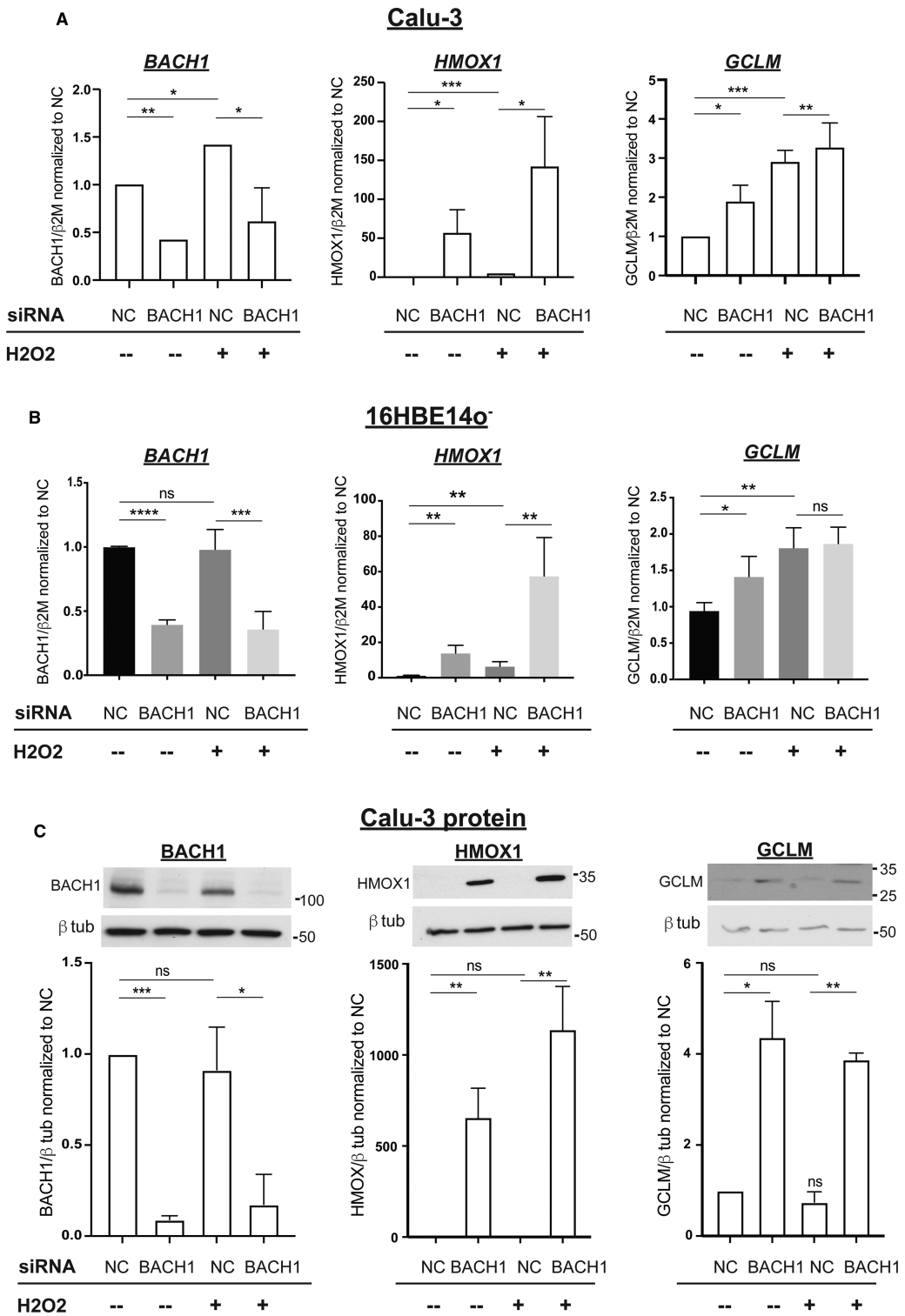

Figure 2. Oxidative stress augments the impact of BACH1 depletion in airway epithelial cells. Part 1 of 2

(**A**) RT-qPCR analysis of *BACH1* (left), *HMOX1* (middle) and *GCLM* (right) expression in Calu-3 cells under four conditions: negative control (NC) siRNA alone, BACH1 siRNA alone, NC siRNA + oxidative stress and BACH1 siRNA + oxidative stress, 48 h after BACH1 depletion followed by 15 h of oxidative stress. (**B**) RT-qPCR analysis of same genes under same conditions as in (**A**) in 16HBE14o$^-$ cells, except 8 h of oxidative stress. β-2-microglobulin (β2M) is the control and the data are normalized to the NC siRNA alone. (**C**) Western blots probed with antibodies specific for BACH1, HMOX1 and GCLM proteins under the

© 2021 The Author(s). This is an open access article published by Portland Press Limited on behalf of the Biochemical Society and distributed under the Creative Commons Attribution License 4.0 (CC BY-NC-ND).

Biochemical Journal (2021) **478** 3741–3756
https://doi.org/10.1042/BCJ20210252

Figure 2. Oxidative stress augments the impact of BACH1 depletion in airway epithelial cells. Part 2 of 2

same conditions as in (**A**) normalized to beta-tubulin (β-tub) control. Western blots were scanned ($n = 3$ for each protein) and signal intensities quantified using ImageJ. Error bars represent SEM and data were analysed by the Student's unpaired *t*-test, ns = not significant, $^{*}P < 0.01$ $^{**}P < 0.001$ $^{***}P < 0.0001$.

in BACH1 but not HMOX1 and GCLM, where oxidative stress alone was not enough to increase protein production (Figure 2C). The combined effect of BACH1 KD and oxidative stress significantly increased protein levels when compared with oxidative stress alone (Figure 2C). Similar protein profiles were seen for 16HBE14o^{-} cell line (Supplementary Figure S3).

Next, we analyzed the effect of BACH1 depletion on *CFTR* mRNA abundance and observed a significant reduction in both 16HBE14o^{-} and Calu-3 cells (Figure 3A and Supplementary Figure S4A, respectively). BACH1 depletion in combination with H_2O_2 stress did not further reduce *CFTR* mRNA levels in either cell line (Figure 3A and Supplementary Figure S4A) and though a greater combined effect on reducing CFTR protein was seen in 16HBE14o^{-} cells, this was not statistically significant across experiments (Figure 3B).

GSH is a major antioxidant in human cells, which is synthesized by glutamate-cysteine ligase (GCL) and a synthetase. The GCL holoenzyme consist of subunits encoded by the *GCLC* and *GCLM* genes [45], both of which are BACH1 regulated according to the DEG list upon BACH1 depletion (Figure 1B and Supplementary Table S1), and reported previously [18]. Since CFTR was shown to be directly involved in GSH transport [28] and *CFTR* mRNA levels may be directly affected by oxidative stress (confirmed here in Calu-3 cells) as a compensatory mechanism to retain high intracellular GSH levels [30], we assessed intracellular GSH levels in BACH1 depleted and H_2O_2 stressed human airway epithelial cells. Though slight increases in intracellular GSH levels were observed in Calu-3 cells upon loss of BACH1, irrespective of H_2O_2 exposure, these effects were not statistically significant in either cell line (Figure 3C and Supplementary Figure S4C).

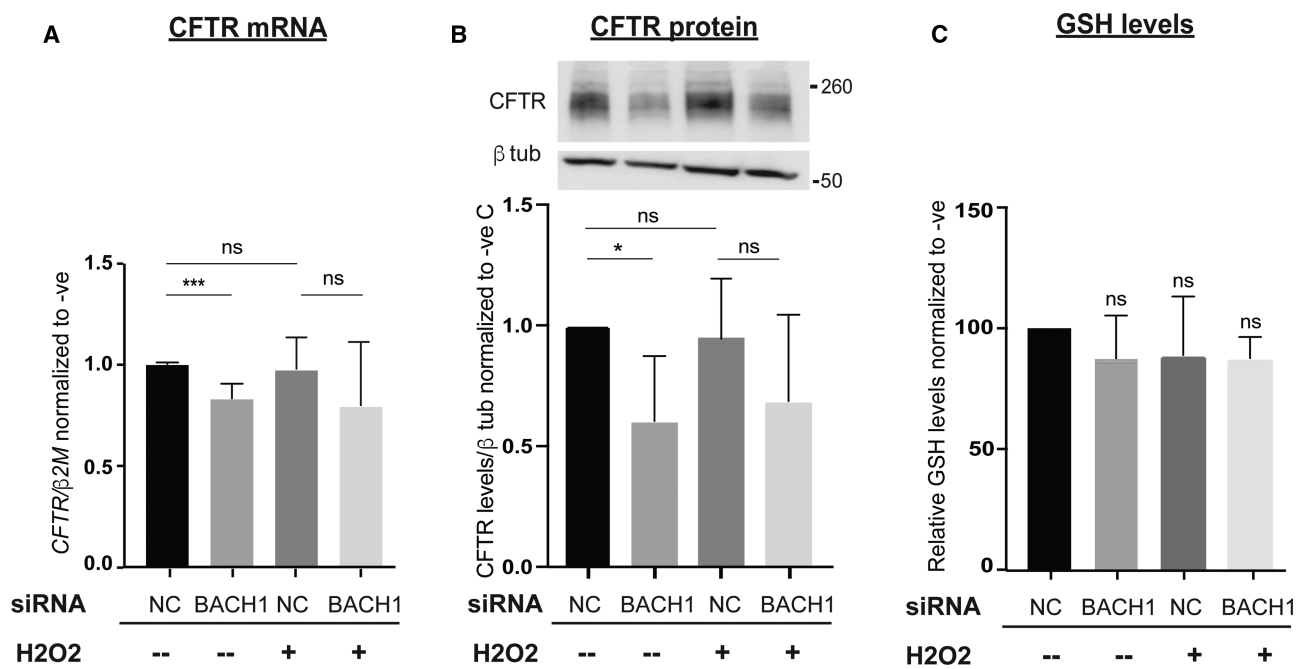

Figure 3. Oxidative stress and the impact of BACH1 depletion on CFTR mRNA and protein in 16HBE14o^{-} cells.

(**A**) RT-qPCR measurements of *CFTR* mRNA levels in 16HBE14o^{-} under same conditions as described in the legend to Figure 2A. β2M is the control and the data are normalized to the NC siRNA alone. (**B**) Western blots probed with antibodies specific to CFTR protein under same conditions as in (**A**) and normalized to β-tubulin. Blots were imaged as in Figure 2C. (**C**) GSH levels after BACH1 depletion normalized to NC siRNA, without or with oxidative stress in 16HBE14o^{-} cells. $N \geq 3$ for all experiments. Error bars represent SEM and data were analysed by the Student's unpaired *t*-test, ns = not significant, $^{*}P < 0.01$ $^{**}P < 0.001$ $^{***}P < 0.0001$.

© 2021 The Author(s). This is an open access article published by Portland Press Limited on behalf of the Biochemical Society and distributed under the Creative Commons Attribution License 4.0 (CC BY-NC-ND).

Biochemical Journal (2021) 478 3741–3756
https://doi.org/10.1042/BCJ20210252

BACH1 occupancy at the *CFTR* locus may be elevated at reduced oxygen levels

Since *CFTR* transcription may be down-regulated upon BACH1 depletion and by oxidative stress independently, and in an airway cell line-specific manner, we next asked whether these mechanisms are acting directly on the *CFTR* locus and/or by indirect mechanisms. It is possible that the increase in the expression of the oxidative stress response genes upon BACH1 inhibition may further repress CFTR levels as an adaptive mechanism [28,30].

To determine if BACH1 directly occupies CREs at the *CFTR* locus in airway epithelial cells we performed chromatin immunoprecipitation followed by deep sequencing (ChIP-seq) with an antibody specific for BACH1, in Calu-3 and 16HBE14o$^-$ cells. Irreproducible discovery rate (IDR) data for biological replicate experiments are shown in Figure 4. A UCSC genome browser graphic of the TAD encompassing the *CFTR* locus, including the 5′ boundary at −80.1 kb from the *CFTR* transcriptional start site to the 3′ boundary at +48.9 kb from the last coding base, is shown for both cell lines (Figure 4A). At the top key *CFTR* CREs are marked and below are peak calls and bigwig files showing BACH1 occupancy. Also shown are open chromatin profiles generated by assay for transposase-accessible chromatin with deep sequencing (ATAC-seq) in both cell lines to illustrate the different CREs utilization in the two airway epithelial lines [7]. In Calu-3 cells, a prominent peak of BACH1 occupancy is seen at the gene promoter and though peaks are evident at the −20.9 and −44 kb CREs, these are not robust enough to be detected by the peak-calling pipeline. In 16HBE14o$^-$ cells, BACH1 promoter occupancy is not called as a peak, nor is that at the −35 kb CRE, however, a peak annotated at the −44 kb CRE confirms our earlier characterization of this element, including by chromatin immunoprecipitation-quantitative PCR (ChIP-qPCR) [10]. Highly significant peaks of BACH1 occupancy observed at or close to the promoters of several of BACH1-regulated genes including *HMOX1*, *GCLM*, *GCLC*, hypoxia inducible factor 1 subunit alpha (*HIF1A*) and *BACH1* demonstrate the efficacy of this BACH1 antibody in ChIP-seq experiments in both the cell lines (Supplementary Figure S5).

Since the physiological levels of oxygen in the lung epithelium are low [46] compared with the levels maintained in standard cell culture incubators, we next asked whether BACH1 occupancy could be enhanced at lower oxygen levels. To answer this, Calu-3 cells were exposed to ambient oxygen levels that were changed from 20% to 8% for 24 h and chromatin then prepared for ChIP-qPCR analysis. The highest occupancy of BACH1 in ChIP-seq was seen at two sites 5′ to the *HMOX1* gene (Supplementary Figure S5), so primers within the most 5′ peak were used to assay BACH1 binding which increased nearly 2 fold at 8% oxygen (Figure 4B). For the *CFTR* regulatory elements at −44 kb, −20.9 kb upstream, the promoter and +6.8 downstream of the gene, very low levels of BACH1 occupancy were detected at 20% O_2 by ChIP-qPCR. Occupancy increased around 2-fold at all these sites when the cells were shifted to 8% O_2. Next, to determine whether increased BACH1 occupancy repressed the expression of its target genes we measured the abundance of mRNA for *HMOX1*, *GCLM*, *GCLC*, *NRF2* (Alternate annotation: *NFE2L2*) and *BACH1* at 20% and 8% ambient oxygen (Figure 4C). For all these genes, increased BACH1 occupancy at their promoters significantly repressed expression. *CFTR* mRNA levels also showed an ∼2-fold reduction in 8% compared with 20% oxygen, consistent with increased BACH1 binding to CREs and at the promoter repressing its expression (Figure 4D). These data suggest that at physiological oxygen concentrations BACH1 acts primarily as a repressor of target gene expression.

BACH1 contributes to chromatin architecture at the *CFTR* locus

The BACH1 BTB domain has the capacity to bind to DNA and may mediate chromatin folding [47]. Moreover, BACH1 was reported earlier to function as an architectural protein at the β-globin locus [31,48]. Building upon these data we used chromatin conformation capture technology (4C-seq) [49], to re-examine the contribution of BACH1 to chromatin looping. We hypothesized that depletion of BACH1 at loci that show changes in expression could be accompanied by an alteration in higher order chromatin structure and looping of CREs. To test this hypothesis, we performed 4C-seq analysis on the *CFTR* locus in Calu-3 cells after BACH1 depletion and compared the results to NC siRNA-treated cells. *CFTR* is located within a TAD, which shows ubiquitous interactions between CTCF sites upstream of the gene at −80.1, −20.9 and downstream at +6.8 and +48.9 kb. Additional looping interactions between enhancers and the gene promoter and the TAD boundaries show cell-type-specificity. Using a viewpoint at the 5′ TAD boundary (−80.1 kb) and comparing the locus architecture after BACH1 depletion with NC siRNA-treated cells, a reduction of interactions with sites between

© 2021 The Author(s). This is an open access article published by Portland Press Limited on behalf of the Biochemical Society and distributed under the Creative Commons Attribution License 4.0 (CC BY-NC-ND).

Biochemical Journal (2021) **478** 3741–3756
https://doi.org/10.1042/BCJ20210252

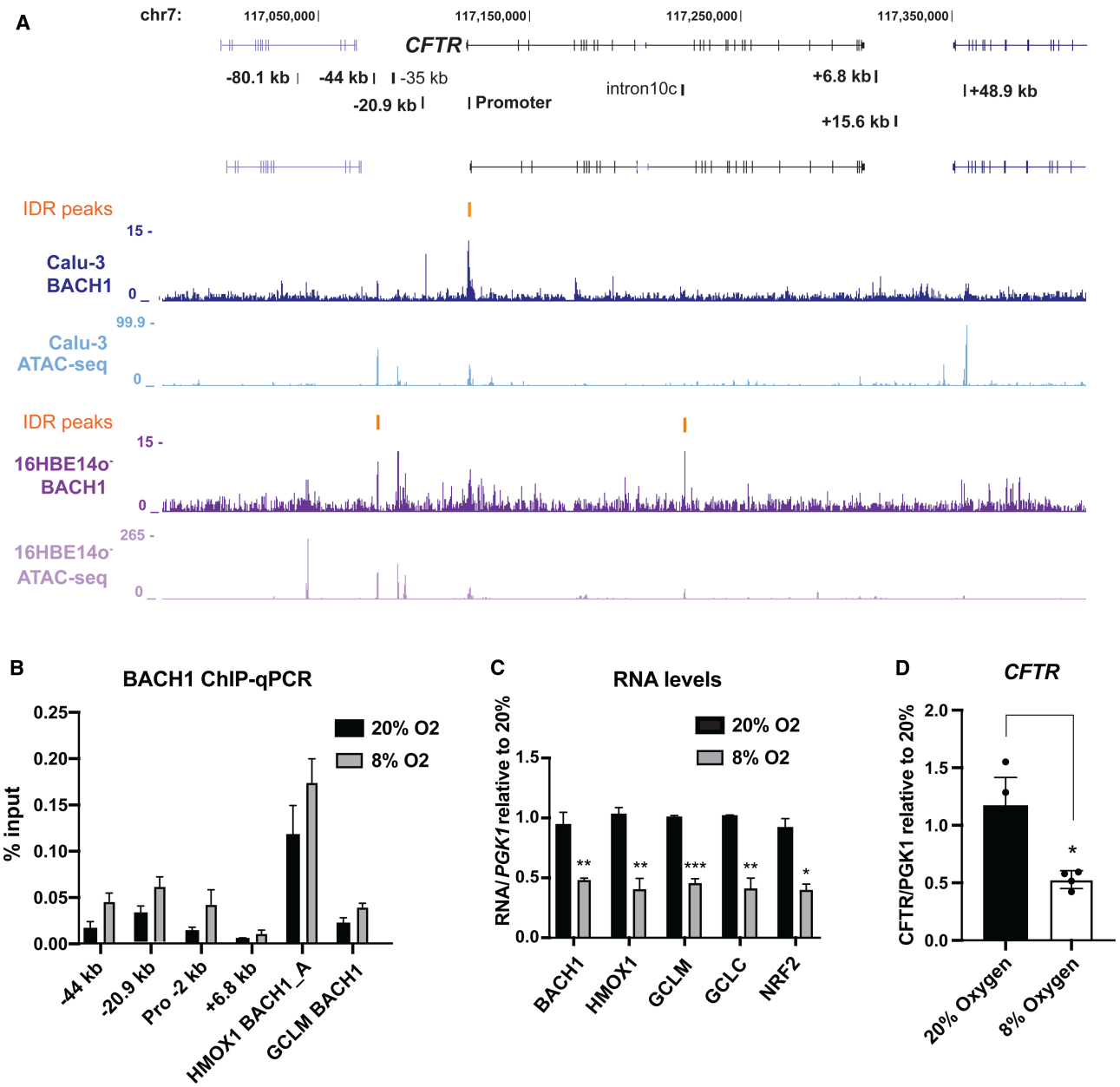

Figure 4. BACH1 occupies the *CFTR* gene promoter or its CREs in Calu-3 and 16HBE14o$^-$ cells, respectively.

(**A**) UCSC genome browser graphic showing the *CFTR* locus within the −80.1 kb to +48.9 kb TAD boundaries. Below sites of BACH1 occupancy determined by ChIP-seq are shown in Calu-3 (blue) and 16HBE14o$^-$ (purple). The ATAC-seq profiles of the same region are shown below each ChIP-seq track for Calu-3 (light blue) and 16HBE14o$^-$ (light purple) cells, respectively. Orange vertical bars denote IDR peak calls. (**B**) ChIP-qPCR analysis of BACH1 occupancy at the −44 kb, −20.9 kb and +6.8 kb CREs and at the *CFTR* promoter in Calu-3 cells under conditions of 20% or 8% oxygen, normalized to the chromatin input levels. *HMOX1* and *GCLM* serve as positive controls for BACH1 occupancy. (**C**) Transcript abundance of genes regulated by BACH1 at 20% and 8% oxygen, measured by RT-qPCR. *PGK1* is the control and data are normalized to the 20% levels. (**D**) *CFTR* transcript levels under 20% or 8% oxygen measured by RT-qPCR as in (**C**). $N \geq 3$ for all experiments. Error bars represent SEM and data were analysed by the Student's unpaired *t*-test, $^*P < 0.01$ $^{**}P < 0.001$ $^{***}P < 0.0001$.

the viewpoint and the gene promoter is seen in the domainogram (Figure 5A, black line and arrow). This loss of interactions is particularly evident at the −44 kb enhancer and the −20.9 kb insulator elements, and was confirmed by the quantitative subtraction analysis track in which loss of interaction is shown above the baseline

© 2021 The Author(s). This is an open access article published by Portland Press Limited on behalf of the Biochemical Society and distributed under the Creative Commons Attribution License 4.0 (CC BY-NC-ND).

Biochemical Journal (2021) **478** 3741–3756
https://doi.org/10.1042/BCJ20210252

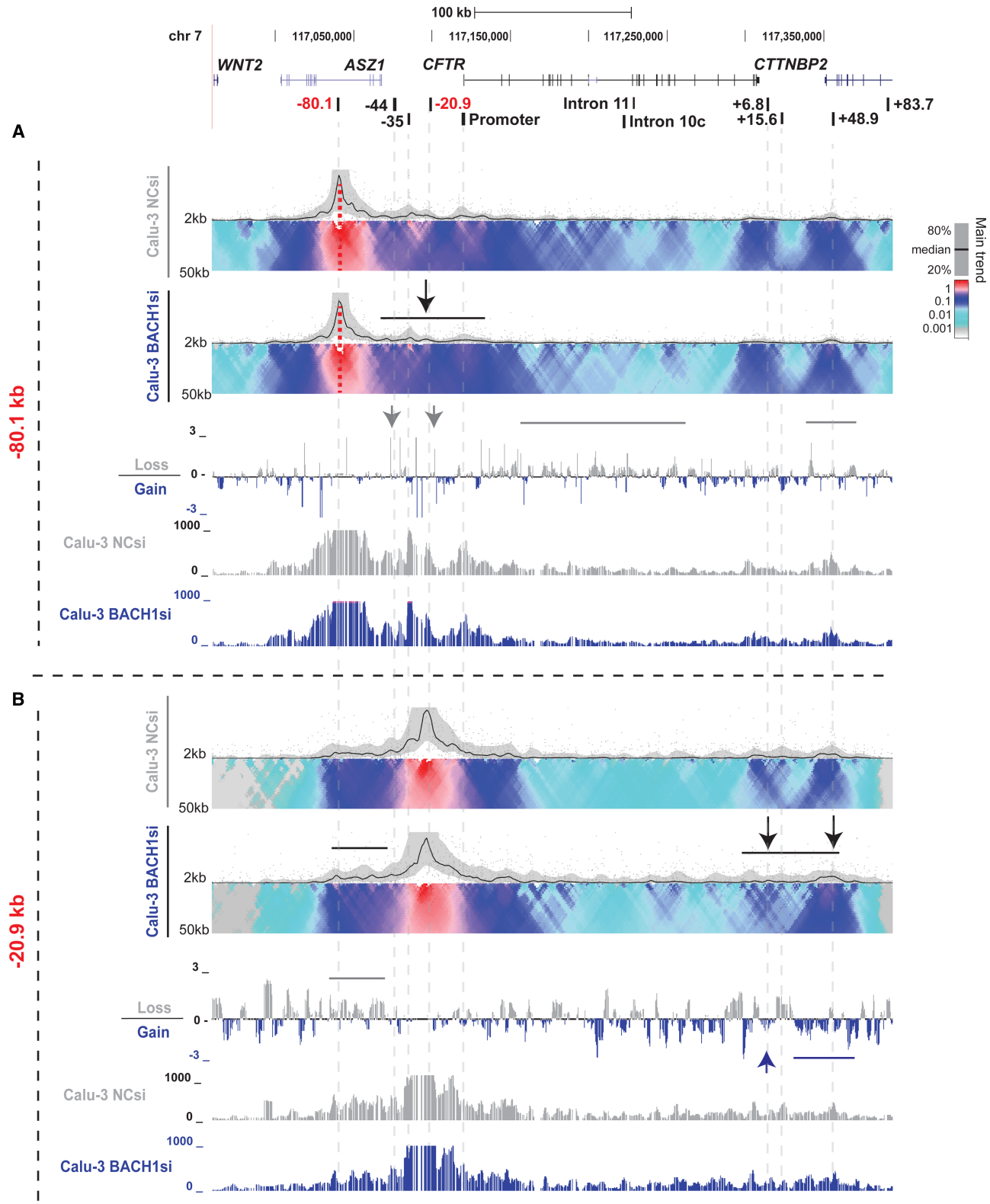

Figure 5. BACH1 depletion alters chromatin architecture at the *CFTR* locus in Calu-3 cells. Part 1 of 2

4C-seq data are shown. At the top is a UCSC genome browser graphic showing the *CFTR* locus within the −80.1 kb to +48.9 kb TAD boundaries. Below 4C-seq data are shown for the −80.1 kb (**A**) and −20.9 kb (**B**) viewpoints after NC siRNA or BACH1 siRNA treatment for 72 h. Black horizontal bars and arrows indicate regions of altered interactions upon BACH1 KD. The 4C-seq data show the main trend of contact profile using a

© 2021 The Author(s). This is an open access article published by Portland Press Limited on behalf of the Biochemical Society and distributed under the Creative Commons Attribution License 4.0 (CC BY-NC-ND).

Biochemical Journal (2021) **478** 3741–3756
https://doi.org/10.1042/BCJ20210252

Figure 5. BACH1 depletion alters chromatin architecture at the *CFTR* locus in Calu-3 cells. Part 2 of 2

5-kb window size as a black line above the domainogram. Relative interactions are normalized to the strongest point (which is set to 1) within each panel. The domainogram uses color-coded intensity values to show relative interactions with window sizes varying from 2 to 50 kb. Here, red denotes the strongest interactions and dark blue, through turquoise, to gray represent decreasing frequencies. Below the domainograms is a track generated by subtracting the BACH1 siRNA peaks from the NC siRNA peaks (.wig files). Gray peaks above the baseline indicate interactions lost upon BACH1 depletion and blue peaks below, those gained. Individual .wig tracks showing quantitative analysis of the 4C-seq interaction data are shown below.

(Figure 5A, gray arrows). The results show that BACH1 depletion disrupts specific aspects of the architecture of the *CFTR* locus, which may correlate with reduced CFTR expression (Figure 1A). In contrast, using a viewpoint at the −20.9 kb 5′ insulator, which recruits CTCF, depletion of BACH1 causes an increase in interactions with 3′ regions particularly the sites of CTCF occupancy at +6.8 kb and the +48.9 kb TAD boundary (Figure 5B, black line and arrows). These increases were confirmed in the quantitative subtraction analysis as blue peaks below the base line (Figure 5B, blue arrows and line). These results suggest an important role for BACH1 in maintenance of CTCF-mediated chromatin looping.

Discussion

Here, we examined the contribution of BACH1 globally to the oxidative stress response in the airway epithelium and also its role in modulating *CFTR* expression. Genome-wide functions of BACH1 revealed by RNA-seq and ChIP-seq analysis in two airway cell lines showed that this factor controlled pathways of cell cycle progression, response to stress and heme binding. Our results are consistent with earlier data in the human embryonic kidney cell line (HEK-293) [18] and suggests the universal involvement of BACH1 in these processes. Additionally, not only does BACH1 bind directly to the *CFTR* locus and to the other loci it represses, it impacts them indirectly through the global effects of modulation of BACH1 and during oxidative stress in airway epithelial cells. Occupancy of BACH1 at CFTR CREs is enhanced at physiological (8%) oxygen levels compared with higher ambient levels in cell culture (20%) and is associated with changes in 3D architecture across the locus. The general mechanisms of *CFTR* regulation by BACH1 were consistent in the two cell lines examined here. Minor variation in response between the lines probably arises due to divergence in their CFTR CRE utilization (Figure 4A). Also relevant may be differences in general physiology in the two airway cell lines, since Calu-3 is a lung adenocarcinoma, while 16HBE14o$^-$ is an SV-40 immortalized cell line.

Glutathione conservation and CF

CFTR expression is both directly and indirectly controlled by the BACH1/NRF2 regulatory axis and oxidative stress. Since the CF lung may be deprived of the normal antioxidant mechanisms due to reduced GSH in the absence of functional CFTR [28–30] the role of BACH1 has added significance. Moreover, abnormal intracellular GSH levels caused by CFTR misregulation may fail to inhibit potential stress-induced apoptosis. By probing the relationship between BACH1 function and oxidative stress in airway cells we revealed the importance of BACH1 inhibition in alleviating oxidative stress by HMOX1. Consistent with our results, in keratinocytes activation of HMOX1 by NRF2 required the inactivation of BACH1 [44]. In contrast, we found that BACH1 did not have a similar effect on GCLM, implicating alternative regulatory mechanisms. The increase in *GCLM* transcript levels under H_2O_2 stress, did not correspond to increased GCLM protein, suggesting complex formation by existing GCLC/GCLM protein modules [50]. No significant changes in intracellular GSH levels were detected in either airway cell line after 24 h of H_2O_2 stress. This could be a result of the cells reaching homeostasis while existing under these conditions. However, recent data showed modulation of the increased levels of BACH1 resulting from increased protein stability in CF cells, did not rescue the decreased HMOX1 levels [51]. This suggests that a defect in the CFTR regulation may have a more complex impact on the BACH1/HMOX1 regulatory axis.

BACH1 and oxygen levels

Binding of BACH1 to the *HMOX1* locus was induced by hypoxia in earlier work [52]. Our data under conditions of reduced oxygen (not hypoxia) showed increased BACH1 binding. Since our ChIP-seq experiments were performed on chromatin purified after routine cell culture in 20% O_2 it is possible that greater BACH1

© 2021 The Author(s). This is an open access article published by Portland Press Limited on behalf of the Biochemical Society and distributed under the Creative Commons Attribution License 4.0 (CC BY-NC-ND).

occupancy might be seen at 8% O_2. Of note, an NRF2-activated ARE was discovered at the 5′ end of *HIF1A* locus in HepG2 and breast cancer cell lines [53] and BACH1 occupancy is seen at this site in Calu-3 cells (Supplementary Figure S5) suggesting that inhibition of BACH1 binding may be essential for NRF2-mediated activation of HIF1A. In this way BACH1 induction following oxidative stress may have an amplified impact and these observations suggest a link between oxidative stress and hypoxia.

Previously, a HIF1-dependent hypoxic repression of CFTR was noted in intestinal cells as a novel compensatory mechanism in regulation of chloride secretion in diarrhea [54]. Other data suggested that in human lung microvascular endothelial cells, CFTR controls not only oxidative stress pathways but also reactive oxygen mediated cell signaling and the inflammatory response. Pharmacological inhibition of CFTR also decreased NRF2, suggesting therapeutic strategies to activate NRF2 may be warranted [55]. In this study, the reduction in NRF2 levels coincided with diminished CFTR, when BACH1 activity was induced at 8% O_2. Therefore, down-regulation of BACH1 might also have therapeutic potential in the airway. The precise cellular mechanisms underlying the dual regulation of CFTR by BACH1 are likely complex. In the Calu-3 cell line used here, we observed no change in BACH1 levels upon oxidative stress alone, suggesting that BACH1 stabilization may be independent of HMOX1 induction or the presence of free heme and/or NRF2 accumulation. Our data also show the direct molecular interactions between BACH1 and CFTR, however, the effect of NRF2/HMOX1 on CFTR could be either dependent or independent of BACH1 regulation. Further studies on the NRF2/HMOX1 regulatory axis may suggest the interdependency of the mechanisms. Recent data on the molecular cross-talk between NRF2, which controls oxidative homeostasis, oxidative stress and regulation of BACH1 degradation in lung cancer are particularly relevant to this topic [56].

BACH1 and chromatin architecture

Our observations that BACH1 depletion alters chromatin architecture at the *CFTR* locus suggest as an intriguing mechanism of gene regulation by this factor. Earlier data [31,48] showed that BACH1 and Mafk proteins can form oligomers via the BTB domain, generating a multimeric DNA binding complex upon recruitment to the MAREs. Moreover, the BTB/POZ domain of Cp190 generates long-range chromosomal contacts in Drosophila, by direct physical interactions with structural elements in the DNA [57,58]. Upon BACH1 depletion, we found a change in the profile of interactions compared with the NC siRNA at known structural elements at the *CFTR* locus, which interact within the TAD. The pattern of interactions supports earlier observations that the binding of BACH1 at several positions at a gene locus triggers the nucleation of an architectural profile, which may be essential for repression of gene expression [31,48]. This suggests a probable mechanism of BACH1 repression followed by NRF2 activation, whereby a different chromatin architecture or conformation can determine the transcriptional status of a gene. Hence, our results extend the functional repertoire of architectural proteins that contribute to higher order chromatin structure and gene expression in airway epithelial cells.

Experimental procedures

Cell culture

Calu-3 cell line was obtained from ATCC and grown in DMEM (Dulbecco's modified Eagle's medium) with 4.5 g/l glucose and 10% FBS (fetal bovine serum). Transformed HBE cell line 16HBE14o$^-$ and was grown in DMEM (1 g/l glucose) with 10% FBS. All cells were grown on plastic at liquid interface.

Cell proliferation assays

The number of viable cells was measured at 8 h and 16 h after exposure to indicated H_2O_2 concentrations after 48 h of initial growth, using the CellTiter96 Aqueous Non-Radioactive Cell Proliferation Assay (MTS; Promega G9241) according to the manufacturer's instructions.

siRNA knockdown and generation of oxidative stress

TF siRNA screen and validation was performed as in [2]. For RNA and protein extraction and GSH assays, 1.2×10^5 Calu-3 or 16HBE14o$^-$ cells were seeded per well in 24 well plates. Calu-3 and 16HBE14o$^-$ cells were reverse or forward transfected, respectively, with BACH1 siRNA (Ambion Silencer®Select Catalog # 4392420-S1860, or Santa Cruz sc-37064) or negative control #2 siRNA (Catalog # 4390846, or Santa Cruz control siRNA-A sc-37007) at 18 pmol/well using Lipofectamine RNAiMAX reagent or Santa Cruz sc-37064, 48 h

© 2021 The Author(s). This is an open access article published by Portland Press Limited on behalf of the Biochemical Society and distributed under the Creative Commons Attribution License 4.0 (CC BY-NC-ND).

Biochemical Journal (2021) 478 3741–3756
https://doi.org/10.1042/BCJ20210252

post-transfection, cells were exposed to oxidative stress by addition of H_2O_2 — 800 μM for 16 h or 600 μM for 8 h for Calu-3 and 16HBE14o$^-$ cells, respectively, in DMEM without serum, before collection of samples.

Reverse transcription quantitative PCR (RT-qPCR)

Total RNA from confluent cultures was extracted with TRIzol (Invitrogen) and cDNA prepared with the TaqMan reverse transcription kit (Invitrogen). SYBR Green PCR mastermix (Thermo) was used for RT-qPCR of all except *CFTR* with primers as in Supplementary Table S2 and normalized to beta 2 microglobulin (β2M) as a housekeeping gene (HKG) control. For RT-qPCR measurements in cells grown under varying O_2 concentrations, *PGK1* was used as the HKG. *CFTR* mRNA levels were assayed using a well-characterized TaqMan assay [2] (Supplementary Table S1) and normalized to β2M as a HKG control.

RNA-seq

RNA-seq (SR 50 bp) was performed as described previously [59] after collection of RNA samples using Trizol (Invitrogen), 72 h upon BACH1 knockdown in Calu-3 cells as described in siRNA knockdown section. Raw reads were aligned with STAR 2.6 (https://github.com/alexdobin/STAR) [60]. Aligned reads were then assigned to genomic features with featureCounts version 1.6.3 in the Subread package (http://subread.sourceforge.net/) [61] and differential gene expression was analyzed using DEseq2 version 1.22.1. (https://www.bioconductor.org/packages/release/bioc/html/DESeq2.html) [62].

Western blotting

To assay the effect of BACH1 depletion on CFTR protein expression, transfections were done as above and at 72 h post-transfection whole cell lysates were collected using NET buffer (20 mM Tris–HCl, pH 7.5, 150 mM NaCl and 1 mM Na_2EDTA) supplemented with Triton-X 100 and protease inhibitors (Sigma). Protein concentration was determined by Bradford assay. SDS- sample loading buffer with β-mercaptoethanol was added and samples were passed through a 25G syringe several times before centrifugation to collect the supernatant. These samples were resolved by SDS–PAGE, transferred to Immobilon membrane and western blots probed with anti-CFTR 596 (Cystic Fibrosis Foundation) and β-tubulin (T4026, Sigma–Aldrich) with ECL detection. Films were scanned by densitometry and the intensities of CFTR were normalized to β-tubulin using ImageJ. For BACH1, HMOX1 and GCLM, the samples were boiled at 95°C for 5 min and 30 μg of protein was blotted with primary antibodies: Rabbit anti-BACH1 (Bethyl Laboratories A303-057A), Rabbit anti-HO-1 (Cell signaling Technology-70081S) and Rabbit anti-GCLM (Genetex-GTX114075), respectively.

Glutathione measurement

GSH colorimetric detection kit from Invitrogen (EIAGSHC) was used to detect intracellular GSH levels in Calu-3 and 16HBE14o$^-$ frozen and washed cell pellets. A freeze–thaw cycle was used to lyse the cells and the kit protocol was followed.

Chromatin immunoprecipitation-quantitative PCR (ChIP-qPCR) and sequencing (ChIP-seq)

ChIP was performed by standard protocols for ChIP-qPCR and ChIP as described in [7]. Antibodies were specific for BACH1 (Bethyl Laboratories A303-057A) for ChIP-seq and ChIP-qPCR or rabbit IgG (Millipore12–370) as control. Chromatin at 8% O_2 levels was collected after cells were shifted from 20% to 8% O_2 for 24 h. The *HPRT1* promoter was used as the HKG control in ChIP-qPCR experiments. Primer sequences used for qPCR are shown in Supplementary Table S3. For ChIP-seq analysis, raw reads were processed using the ENCODE Transcription Factor and Histone ChIP-Seq processing pipeline (https://github.com/ENCODE-DCC/ChIP-seq-pipeline2) according to the ENCODE (phase-3) guidelines on the hg19 reference genome. This includes mapping using BWA [63] and peak calling with MACS2 [64]. Peak data were filtered using and processed for motif distribution using HOMER (4.7.2q) (http://homer.ucsd.edu/homer/index.html) [65].

Circular chromosome conformation capture—4c-seq

7.8×10^6 Calu-3 cells were reverse transfected using BACH1 siRNA or Negative control #2 siRNA as described above in 10 cm dishes and pellets prepared according to protocol described in [49,66] after 72 h of transfection. 4C-seq libraries were generated from cultured cells as described in [49]. NlaIII and DpnII or Csp6I were used

© 2021 The Author(s). This is an open access article published by Portland Press Limited on behalf of the Biochemical Society and distributed under the Creative Commons Attribution License 4.0 (CC BY-NC-ND).

as the primary or secondary restriction enzymes, respectively. Enzyme pairs and primer sequences used to generate 4C-seq libraries for each viewpoint are shown in Supplementary Table S4. The sequencing data were processed using the 4C-seq pipe protocol. All 4C-seq images were generated using default parameters of the pipeline as per [66]. 4C-seq was quantified and mapped using the pipe4C processing pipeline [49]. Raw reads were aligned to the hg19 genome using Bowtie2 v4.8.3 and sorted using SAMtools v1.3. Bigwig subtraction tracks were generated using deepTools bigwigCompare [67] with default settings.

Statistics

Error bars in all graphs denote standard error of the mean (SEM). Statistical analysis used the Student's unpaired *t*-tests in Prism software (GraphPad). $*P < 0.01$ $**P < 0.001$ $***P < 0.0001$.

Footnote: * This manuscript uses legacy nomenclature for the *CFTR* gene to be consistent with our earlier work.

Data Availability

The datasets produced in this study are available at GEO GSE165719.

Competing Interests

The authors declare that there are no competing interests associated with the manuscript.

Funding

This work was supported by the National Institutes of Health [R01 HL094585; HL117843] (AH), and the Cystic Fibrosis Foundation [Harris 16G0, 15/17XX0 and18P0].

Open Access

Open access for this article was enabled by the participation of Case Western Reserve University in an all-inclusive *Read & Publish* pilot with Portland Press and the Biochemical Society under a transformative agreement with EBSCO.

Acknowledgements

We thank Dr. Peter Krijger for advice on the 4C-seq protocol; Dr Pieter Faber and staff at the University of Chicago Genomics Core for all deep sequencing; also the CWRU genomics core for some 4C-seq sequencing.

CRediT Author Contribution

Ann Harris: Conceptualization, Resources, Data curation, Formal analysis, Supervision, Funding acquisition, Validation, Writing — original draft, Project administration, Writing — review and editing. **Monali NandyMazumdar**: Conceptualization, Resources, Data curation, Formal analysis, Validation, Investigation, Visualization, Methodology, Writing — original draft, Writing — review and editing. **Alekh Paranjapye**: Resources, Data curation, Formal analysis, Validation, Investigation, Methodology, Writing — review and editing. **James Browne**: Resources, Data curation, Formal analysis, Validation, Investigation, Methodology, Writing — review and editing. **Shiyi Yin**: Data curation, Software, Formal analysis, Visualization. **Shih-Hsing Leir**: Resources, Supervision, Methodology, Writing — review and editing.

Abbreviations

ABCC2, ATP-binding cassette subfamily C member 2; ARE, antioxidant response elements; BACH1, BTB domain and CNC homolog 1; CF, cystic fibrosis; *CFTR*, cystic fibrosis transmembrane conductance regulator; ChIP-qPCR, chromatin immunoprecipitation- quantitative PCR; CREs, *cis*-regulatory elements; *DDAH1*, dimethylarginine dimethylaminohydrolase 1; DEGs, differentially expressed genes; DMEM, Dulbecco's modified Eagle's medium; FBS, fetal bovine serum; GCL, glutamate-cysteine ligase; *GCLC*, glutamate-cysteine ligase catalytic; *GCLM*, glutamate-cysteine ligase modifier; GSH, glutathione; HBE, human bronchial epithelial; *HIF1A*, hypoxia inducible factor 1 subunit alpha; HKG, housekeeping gene; *HMOX1*, heme oxygenase 1; MAREs, Maf recognition elements; NC, negative control; ROS, reactive oxygen species; TAD, topologically-associated domain; TFs, transcription factors; *TPRG1L*, tumor protein p63 regulated 1 like.

© 2021 The Author(s). This is an open access article published by Portland Press Limited on behalf of the Biochemical Society and distributed under the Creative Commons Attribution License 4.0 (CC BY-NC-ND).

Biochemical Journal (2021) **478** 3741–3756
https://doi.org/10.1042/BCJ20210252

References

1 Lambert, S.A., Jolma, A., Campitelli, L.F., Das, P.K., Yin, Y., Albu, M. et al. (2018) The human transcription factors. *Cell* **172**, 650–665 https://doi.org/10.1016/j.cell.2018.01.029

2 Mutolo, M.J., Leir, S.H., Fossum, S.L., Browne, J.A. and Harris, A. (2018) A transcription factor network represses CFTR gene expression in airway epithelial cells. *Biochem. J.* **475**, 1323–1334 https://doi.org/10.1042/BCJ20180044

3 Roeder, R.G. (2019) 50+ years of eukaryotic transcription: an expanding universe of factors and mechanisms. *Nat. Struct. Mol. Biol.* **26**, 783–791 https://doi.org/10.1038/s41594-019-0287-x

4 Smith, E.M., Lajoie, B.R., Jain, G. and Dekker, J. (2016) Invariant TAD boundaries constrain cell-type-specific looping interactions between promoters and distal elements around the CFTR locus. *Am. J. Hum. Genet.* **98**, 185–201 https://doi.org/10.1016/j.ajhg.2015.12.002

5 Gosalia, N. and Harris, A. (2015) Chromatin dynamics in the regulation of CFTR expression. *Genes (Basel)* **6**, 543–558 https://doi.org/10.3390/genes6030543

6 Gosalia, N., Neems, D., Kerschner, J.L., Kosak, S.T. and Harris, A. (2014) Architectural proteins CTCF and cohesin have distinct roles in modulating the higher order structure and expression of the CFTR locus. *Nucleic Acids Res.* **42**, 9612–9622 https://doi.org/10.1093/nar/gku648

7 NandyMazumdar, M., Yin, S., Paranjapye, A., Kerschner, J.L., Swahn, H., Ge, A. et al. (2020) Looping of upstream cis-regulatory elements is required for CFTR expression in human airway epithelial cells. *Nucleic Acids Res.* **48**, 3513–3524 https://doi.org/10.1093/nar/gkaa089

8 Blackledge, N.P., Carter, E.J., Evans, J.R., Lawson, V., Rowntree, R.K. and Harris, A. (2007) CTCF mediates insulator function at the CFTR locus. *Biochem. J.* **408**, 267–275 https://doi.org/10.1042/BJ20070429

9 Zhang, Z., Leir, S.H. and Harris, A. (2013) Immune mediators regulate CFTR expression through a bifunctional airway-selective enhancer. *Mol. Cell. Biol.* **33**, 2843–2853 https://doi.org/10.1128/MCB.00003-13

10 Zhang, Z., Leir, S.H. and Harris, A. (2015) Oxidative stress regulates CFTR gene expression in human airway epithelial cells through a distal antioxidant response element. *Am. J. Respir. Cell Mol. Biol.* **52**, 387–396 https://doi.org/10.1165/rcmb.2014-0263OC

11 Gallant, S. and Gilkeson, G. (2006) ETS transcription factors and regulation of immunity. *Arch. Immunol. Ther. Exp. (Warsz)* **54**, 149–163 https://doi.org/10.1007/s00005-006-0017-z

12 Latchman, D.S. (1996) Activation and repression of gene expression by POU family transcription factors. *Philos. Trans. R. Soc. Lond. B Biol. Sci.* **351**, 511–515 https://doi.org/10.1098/rstb.1996.0049

13 Ramakrishnan, A.B., Sinha, A., Fan, V.B. and Cadigan, K.M. (2018) The Wnt transcriptional switch: TLE removal or inactivation? *Bioessays* **10**, 1002 PMID: 29250807

14 Zhang, X., Guo, J., Wei, X., Niu, C., Jia, M., Li, Q. et al. (2018) Bach1: function, regulation, and involvement in disease. *Oxidative Med. Cell. Longev.* **2018**, 1347969 https://doi.org/10.1155/2018/1347969

15 Oyake, T., Itoh, K., Motohashi, H., Hayashi, N., Hoshino, H., Nishizawa, M. et al. (1996) Bach proteins belong to a novel family of BTB-basic leucine zipper transcription factors that interact with MafK and regulate transcription through the NF-E2 site. *Mol. Cell. Biol.* **16**, 6083–6095 https://doi.org/10.1128/MCB.16.11.6083

16 Zhou, Y., Wu, H., Zhao, M., Chang, C. and Lu, Q. (2016) The Bach family of transcription factors: a comprehensive review. *Clin. Rev. Allergy Immunol.* **50**, 345–356 https://doi.org/10.1007/s12016-016-8538-7

17 Raghunath, A., Sundarraj, K., Nagarajan, R., Arfuso, F., Bian, J., Kumar, A.P. et al. (2018) Antioxidant response elements: discovery, classes, regulation and potential applications. *Redox Biol.* **17**, 297–314 https://doi.org/10.1016/j.redox.2018.05.002

18 Warnatz, H.J., Schmidt, D., Manke, T., Piccini, I., Sultan, M., Borodina, T. et al. (2011) The BTB and CNC homology 1 (BACH1) target genes are involved in the oxidative stress response and in control of the cell cycle. *J. Biol. Chem.* **286**, 23521–23532 https://doi.org/10.1074/jbc.M111.220178

19 Arunachalam, A., Lakshmanan, D.K., Ravichandran, G., Paul, S., Manickam, S., Kumar, P.V. et al. (2021) Regulatory mechanisms of heme regulatory protein BACH1: a potential therapeutic target for cancer. *Med. Oncol.* **38**, 122 https://doi.org/10.1007/s12032-021-01573-z

20 Cohen, B., Tempelhof, H., Raz, T., Oren, R., Nicenboim, J., Bochner, F. et al. (2020) BACH family members regulate angiogenesis and lymphangiogenesis by modulating VEGFC expression. *Life Sci. Alliance* **3**, e202000666 https://doi.org/10.26508/lsa.202000666

21 Yusoff, F.M., Maruhashi, T., Kawano, K.I., Nakashima, A., Chayama, K., Tashiro, S. et al. (2021) Bach1 plays an important role in angiogenesis through regulation of oxidative stress. *Microvasc. Res.* **134**, 104126 https://doi.org/10.1016/j.mvr.2020.104126

22 Anderson, N.M. and Simon, M.C. (2019) BACH1 orchestrates lung cancer metastasis. *Cell* **178**, 265–267 https://doi.org/10.1016/j.cell.2019.06.020

23 Liang, Y., Wu, H., Lei, R., Chong, R.A., Wei, Y., Lu, X. et al. (2012) Transcriptional network analysis identifies BACH1 as a master regulator of breast cancer bone metastasis. *J. Biol. Chem.* **287**, 33533–33544 https://doi.org/10.1074/jbc.M112.392332

24 Sato, M., Matsumoto, M., Saiki, Y., Alam, M., Nishizawa, H., Rokugo, M. et al. (2020) BACH1 promotes pancreatic cancer metastasis by repressing epithelial genes and enhancing epithelial-mesenchymal transition. *Cancer Res.* **80**, 1279–1292 https://doi.org/10.1158/0008-5472.CAN-18-4099

25 Zhu, G.D., Liu, F., OuYang, S., Zhou, R., Jiang, F.N., Zhang, B. et al. (2018) BACH1 promotes the progression of human colorectal cancer through BACH1/CXCR4 pathway. *Biochem. Biophys. Res. Commun.* **499**, 120–127 https://doi.org/10.1016/j.bbrc.2018.02.178

26 Padilla, J. and Lee, J. (2021) A novel therapeutic target, BACH1, regulates cancer metabolism. *Cells* **10**, 634 https://doi.org/10.3390/cells10030634

27 Park, H.S., Kim, S.R. and Lee, Y.C. (2009) Impact of oxidative stress on lung diseases. *Respirology* **14**, 27–38 https://doi.org/10.1111/j.1440-1843.2008.01447.x

28 Linsdell, P. and Hanrahan, J.W. (1998) Glutathione permeability of CFTR. *Am. J. Physiol.* **275**, C323–C326 https://doi.org/10.1152/ajpcell.1998.275.1.C323

29 Kogan, I., Ramjeesingh, M., Li, C., Kidd, J.F., Wang, Y., Leslie, E.M. et al. (2003) CFTR directly mediates nucleotide-regulated glutathione flux. *EMBO J.* **22**, 1981–1989 https://doi.org/10.1093/emboj/cdg194

30 Cantin, A.M., Bilodeau, G., Ouellet, C., Liao, J. and Hanrahan, J.W. (2006) Oxidant stress suppresses CFTR expression. *Am. J. Physiol. Cell Physiol.* **290**, C262–C270 https://doi.org/10.1152/ajpcell.00070.2005

31 Yoshida, C., Tokumasu, F., Hohmura, K.I., Bungert, J., Hayashi, N., Nagasawa, T. et al. (1999) Long range interaction of cis-DNA elements mediated by architectural transcription factor Bach1. *Genes Cells* **4**, 643–655 https://doi.org/10.1046/j.1365-2443.1999.00291.x

32 Browne, J.A., NandyMazumdar, M., Paranjapye, A., Leir, S.H. and Harris, A. (2021) The bromodomain containing 8 (BRD8) transcriptional network in human lung epithelial cells. *Mol. Cell. Endocrinol.* **524**, 111169 https://doi.org/10.1016/j.mce.2021.111169

© 2021 The Author(s). This is an open access article published by Portland Press Limited on behalf of the Biochemical Society and distributed under the Creative Commons Attribution License 4.0 (CC BY-NC-ND).

33 Paranjapye, A., Mutolo, M.J., Ebron, J.S., Leir, S.H. and Harris, A. (2020) The FOXA1 transcriptional network coordinates key functions of primary human airway epithelial cells. *Am. J. Physiol. Lung Cell. Mol. Physiol.* **319**, L126–LL36 https://doi.org/10.1152/ajplung.00023.2020
34 Reimand, J., Kull, M., Peterson, H., Hansen, J. and Vilo, J. (2007) G:Profiler–a web-based toolset for functional profiling of gene lists from large-scale experiments. *Nucleic Acids Res.* **35**, W193-200 https://doi.org/10.1093/nar/gkm226
35 Vollrath, V., Wielandt, A.M., Iruretagoyena, M. and Chianale, J. (2006) Role of Nrf2 in the regulation of the Mrp2 (ABCC2) gene. *Biochem. J.* **395**, 599–609 https://doi.org/10.1042/BJ20051518
36 Zhao, C., Li, T., Han, B., Yue, W., Shi, L., Wang, H. et al. (2016) DDAH1 deficiency promotes intracellular oxidative stress and cell apoptosis via a miR-21-dependent pathway in mouse embryonic fibroblasts. *Free Radic. Biol. Med.* **92**, 50–60 https://doi.org/10.1016/j.freeradbiomed.2016.01.015
37 Sun, J., Hoshino, H., Takaku, K., Nakajima, O., Muto, A., Suzuki, H. et al. (2002) Hemoprotein Bach1 regulates enhancer availability of heme oxygenase-1 gene. *EMBO J.* **21**, 5216–5224 https://doi.org/10.1093/emboj/cdf516
38 Askew, D.J. and Silverman, G.A. (2008) Intracellular and extracellular serpins modulate lung disease. *J. Perinatol.* **28**, S127–S135 https://doi.org/10.1038/jp.2008.150
39 Law, R.H., Zhang, Q., McGowan, S., Buckle, A.M., Silverman, G.A., Wong, W. et al. (2006) An overview of the serpin superfamily. *Genome Biol.* **7**, 216 https://doi.org/10.1186/gb-2006-7-5-216
40 Anttila, S., Raunio, H. and Hakkola, J. (2011) Cytochrome P450-mediated pulmonary metabolism of carcinogens: regulation and cross-talk in lung carcinogenesis. *Am. J. Respir. Cell Mol. Biol.* **44**, 583–590 https://doi.org/10.1165/rcmb.2010-0189RT
41 Chaoyang, Y., Qingfeng, B. and Jinxing, F. (2019) MiR-216a-5p protects 16HBE cells from H_2O_2-induced oxidative stress through targeting HMGB1/NF-kB pathway. *Biochem. Biophys. Res. Commun.* **508**, 416–420 https://doi.org/10.1016/j.bbrc.2018.11.060
42 Wijeratne, S.S., Cuppett, S.L. and Schlegel, V. (2005) Hydrogen peroxide induced oxidative stress damage and antioxidant enzyme response in Caco-2 human colon cells. *J. Agric. Food Chem.* **53**, 8768–8774 https://doi.org/10.1021/jf0512003
43 Keyse, S.M., Applegate, L.A., Tromvoukis, Y. and Tyrrell, R.M. (1990) Oxidant stress leads to transcriptional activation of the human heme oxygenase gene in cultured skin fibroblasts. *Mol. Cell. Biol.* **10**, 4967–4969 https://doi.org/10.1128/mcb.10.9.4967-4969.1990
44 Reichard, J.F., Motz, G.T. and Puga, A. (2007) Heme oxygenase-1 induction by NRF2 requires inactivation of the transcriptional repressor BACH1. *Nucleic Acids Res.* **35**, 7074–7086 https://doi.org/10.1093/nar/gkm638
45 Lee, J.I., Kang, J. and Stipanuk, M.H. (2006) Differential regulation of glutamate-cysteine ligase subunit expression and increased holoenzyme formation in response to cysteine deprivation. *Biochem. J.* **393**(Pt 1), 181–190 https://doi.org/10.1042/BJ20051111
46 McKeown, S.R. (2014) Defining normoxia, physoxia and hypoxia in tumours-implications for treatment response. *Br. J. Radiol.* **87**, 20130676 https://doi.org/10.1259/bjr.20130676
47 Albagli, O., Dhordain, P., Deweindt, C., Lecocq, G. and Leprince, D. (1995) The BTB/POZ domain: a new protein-protein interaction motif common to DNA- and actin-binding proteins. *Cell Growth Differ.* **6**, 1193–1198 PMID: 8519696
48 Igarashi, K., Hoshino, H., Muto, A., Suwabe, N., Nishikawa, S., Nakauchi, H. et al. (1998) Multivalent DNA binding complex generated by small Maf and Bach1 as a possible biochemical basis for beta-globin locus control region complex. *J. Biol. Chem.* **273**, 11783–11790 https://doi.org/10.1074/jbc.273.19.11783
49 Krijger, P.H.L., Geeven, G., Bianchi, V., Hilvering, C.R.E. and de Laat, W. (2020) 4C-seq from beginning to end: a detailed protocol for sample preparation and data analysis. *Methods* **170**, 17–32 https://doi.org/10.1016/j.ymeth.2019.07.014
50 Franklin, C.C., Backos, D.S., Mohar, I., White, C.C., Forman, H.J. and Kavanagh, T.J. (2009) Structure, function, and post-translational regulation of the catalytic and modifier subunits of glutamate cysteine ligase. *Mol. Aspects Med.* **30**, 86–98 https://doi.org/10.1016/j.mam.2008.08.009
51 Chillappagari, S., Garapati, V., Mahavadi, P., Naehrlich, L., Schmeck, B.T., Schmitz, M.L. et al. (2020) Defective BACH1/HO-1 regulatory circuits in cystic fibrosis bronchial epithelial cells. *J. Cyst. Fibros* **S1569-1993**, 30150–8 PMID: 32534959
52 Kitamuro, T., Takahashi, K., Ogawa, K., Udono-Fujimori, R., Takeda, K., Furuyama, K. et al. (2003) Bach1 functions as a hypoxia-inducible repressor for the heme oxygenase-1 gene in human cells. *J. Biol. Chem.* **278**, 9125–9133 https://doi.org/10.1074/jbc.M209939200
53 Lacher, S.E., Levings, D.C., Freeman, S. and Slattery, M. (2018) Identification of a functional antioxidant response element at the HIF1A locus. *Redox Biol.* **19**, 401–411 https://doi.org/10.1016/j.redox.2018.08.014
54 Zheng, W., Kuhlicke, J., Jackel, K., Eltzschig, H.K., Singh, A., Sjoblom, M. et al. (2009) Hypoxia inducible factor-1 (HIF-1)-mediated repression of cystic fibrosis transmembrane conductance regulator (CFTR) in the intestinal epithelium. *FASEB J.* **23**, 204–213 https://doi.org/10.1096/fj.08-110221
55 Khalaf, M., Scott-Ward, T., Causer, A., Saynor, Z., Shepherd, A., Gorecki, D. et al. (2020) Cystic fibrosis transmembrane conductance regulator (CFTR) in human lung microvascular endothelial cells controls oxidative stress, reactive oxygen-mediated cell signaling and inflammatory responses. *Front. Physiol.* **11**, 879 https://doi.org/10.3389/fphys.2020.00879
56 Lignitto, L., LeBoeuf, S.E., Homer, H., Jiang, S., Askenazi, M., Karakousi, T.R. et al. (2019) Nrf2 activation promotes lung cancer metastasis by inhibiting the degradation of Bach1. *Cell* **178**, 316–329.e18 https://doi.org/10.1016/j.cell.2019.06.003
57 Oliver, D., Sheehan, B., South, H., Akbari, O. and Pai, C.Y. (2010) The chromosomal association/dissociation of the chromatin insulator protein Cp190 of *Drosophila melanogaster* is mediated by the BTB/POZ domain and two acidic regions. *BMC Cell Biol.* **11**, 101 https://doi.org/10.1186/1471-2121-11-101
58 Vogelmann, J., Le Gall, A., Dejardin, S., Allemand, F., Gamot, A., Labesse, G. et al. (2014) Chromatin insulator factors involved in long-range DNA interactions and their role in the folding of the Drosophila genome. *PLoS Genet.* **10**, e1004544 https://doi.org/10.1371/journal.pgen.1004544
59 Browne, J.A., Yang, R., Eggener, S.E., Leir, S.H. and Harris, A. (2016) HNF1 regulates critical processes in the human epididymis epithelium. *Mol. Cell. Endocrinol.* **425**, 94–102 https://doi.org/10.1016/j.mce.2016.01.021
60 Dobin, A., Davis, C.A., Schlesinger, F., Drenkow, J., Zaleski, C., Jha, S. et al. (2013) STAR: ultrafast universal RNA-seq aligner. *Bioinformatics* **29**, 15–21 https://doi.org/10.1093/bioinformatics/bts635
61 Liao, Y., Smyth, G.K. and Shi, W. (2014) Featurecounts: an efficient general purpose program for assigning sequence reads to genomic features. *Bioinformatics* **30**, 923–930 https://doi.org/10.1093/bioinformatics/btt656
62 Love, M.I., Huber, W. and Anders, S. (2014) Moderated estimation of fold change and dispersion for RNA-seq data with DESeq2. *Genome Biol.* **15**, 550 https://doi.org/10.1186/s13059-014-0550-8

© 2021 The Author(s). This is an open access article published by Portland Press Limited on behalf of the Biochemical Society and distributed under the Creative Commons Attribution License 4.0 (CC BY-NC-ND).

Biochemical Journal (2021) **478** 3741–3756
https://doi.org/10.1042/BCJ20210252

63 Li, H. and Durbin, R. (2009) Fast and accurate short read alignment with Burrows-Wheeler transform. *Bioinformatics* **25**, 1754–1760 https://doi.org/10.1093/bioinformatics/btp324
64 Zhang, Y., Liu, T., Meyer, C.A., Eeckhoute, J., Johnson, D.S., Bernstein, B.E. et al. (2008) Model-based analysis of ChIP-Seq (MACS). *Genome Biol.* **9**, R137 https://doi.org/10.1186/gb-2008-9-9-r137
65 Heinz, S., Benner, C., Spann, N., Bertolino, E., Lin, Y.C., Laslo, P. et al. (2010) Simple combinations of lineage-determining transcription factors prime cis-regulatory elements required for macrophage and B cell identities. *Mol. Cell* **38**, 576–589 https://doi.org/10.1016/j.molcel.2010.05.004
66 Splinter, E., de Wit, E., van de Werken, H.J., Klous, P. and de Laat, W. (2012) Determining long-range chromatin interactions for selected genomic sites using 4C-seq technology: from fixation to computation. *Methods* **58**, 221–230 https://doi.org/10.1016/j.ymeth.2012.04.009
67 Ramirez, F., Ryan, D.P., Gruning, B., Bhardwaj, V., Kilpert, F., Richter, A.S. et al. (2016) Deeptools2: a next generation web server for deep-sequencing data analysis. *Nucleic Acids Res.* **44**, W160–W165 https://doi.org/10.1093/nar/gkw257
68 Raudvere, U., Kolberg, L., Kuzmin, I., Arak, T., Adler, P., Peterson, H. et al. (2019) G:Profiler: a web server for functional enrichment analysis and conversions of gene lists (2019 update). *Nucleic Acids Res.* **47**, W191–W1W8 https://doi.org/10.1093/nar/gkz369

© 2021 The Author(s). This is an open access article published by Portland Press Limited on behalf of the Biochemical Society and distributed under the Creative Commons Attribution License 4.0 (CC BY-NC-ND).